International Journal of Mechanical, Industrial and Aerospace Sciences
ISSN: 2517-9950
Vol:9, No:7, 2015

Characterization of the Dispersion Phenomenon in an Optical Biosensor

An-Shik Yang, Chin-Ting Kuo, Yung-Chun Yang, Wen-Hsin Hsieh, Chiang-Ho Cheng

***Abstract*—**Optical biosensors have become a powerful detection and analysis tool for wide-ranging applications in biomedical research, pharmaceuticals and environmental monitoring. This study carried out the computational fluid dynamics (CFD)-based simulations to explore the dispersion phenomenon in the micro channel of an optical biosensor. The predicted time sequences of concentration contours were utilized to better understand the dispersion development occurred in different geometric shapes of micro channels. The simulation results showed the surface concentrations at the sensing probe (with the best performance of a grating coupler) in respect of time to appraise the dispersion effect and therefore identify the design configurations resulting in minimum dispersion.

***Keywords*—**CFD simulations, dispersion, microfluidic, optical waveguide sensors.

I. Introduction

OPTICAL biosensors have become increasingly important as an detection and analysis device for various chemical, biological and medical applications [1]. A number of design arrangements combining micro channels with electrical and optical elements have been proposed to perform high-precision downscale biochemical sensing assays with enhanced detection sensitivities, reduced analysis time and test sample volume in the study fields of healthcare, food, environmental monitoring, clinical diagnostics and pharmaceuticals [2]-[5]. At the present time, label-free bioassay technologies have attracted much attention with different types of label-free biosensors formed to achieve high sensitivity as compared to fluorescence based measurements. Goral et al. developed a label-free resonant waveguide grating biosensor system to sense ligand-directed functional selectivity acting on G protein-coupled receptors [6]. Kumeria et al. also demonstrated a label-free reflectometric interference spectroscopy microchip biosensor for recognizing circulating tumor cells [7]. To provide a feasible alternative for rapid screening of toxins in agriculture products and foods, Xu et al. devised a label-free optical biosensor using gold nanorods as a sensing platform for detection of aflatoxin B1 [8]. Zhang et al. manufactured an effective porous silicon microcavity on silicon-on-insulator wafer with impressive sensitivity and fast response for good DNA sensing performance [9]. Subsequently, Orgovan et al. illustrated the capabilities of innovative optical waveguide lightmode spectroscopy to monitor adhesion and spreading properties of primary monocytes inaccessible from human blood with sensitivity [10]. Zhang et al. used a photonic crystal structure in a total-internal-reflection configuration to produce a label-free biosensor for quick and accurate assays of Troponin I concentrations (considered as a cardiac biomarker) in the blood samples from patients during clinical settings [11].

The extent of portable fully-packaged optical biosensors has been significantly condensed via integration of chip-compatible sample handling structures [12]. The label-free grating coupler sensors use a grating to stimulate the guided modes of a planar waveguide with incident plane-polarized laser diffracted from the grating and initiated to transmit through internal reflections within the waveguide [13]. The sensors then measure changes in the refractive index with high sensitivity attributable to the deposition of biomolecules on the waveguide [14]. However, the laminar velocity profiles in micro channel systems basically cause substantial axial dispersion that can have an unfavorable influence on radial concentration uniformity. Hence, the radial variations in concentration can result in the mean concentration over the channel cross section greater than the concentration at the sensing surface in contact with the catalyst. For such a case, the concentration difference is likely to cause inaccuracies in the kinetic measurements [15]. In this study, the computational analysis was utilized to investigate the dispersion behavior in a grating coupled optical sensor having the new design of a cross-shaped micro channel. Different geometric configurations of the flow channel were tested to identify the conditions leading to minimization of the dispersion effect.

II. Device Design and Fabrication

Fig. 1 demonstrates the schematics of optical sensors having (a) the conventional micro channel and (b) the proposed cross-shaped micro channel. The microfluidic channel was made of cyclic olefin copolymer (COC) with the associated design and fabrication methods described below.

In this research, we also proposed four modified models of cross-shaped micro channels with the major difference in the angles between two inlets. Fig. 2 illustrates the schematics of optical sensors with the cross-shaped micro channel designs at the angles of (a) 60°, (b) 90°, (c) 120° and (d) 180°, respectively. In practice, COC is highly transparent, chemical-resistant and

An-Shik Yang and Chin-Ting Kuo are with Department of Energy and Refrigerating Air-Conditioning Engineering, National Taipei University of Technology, Taipei 10608, Taiwan (phone: 886-2-2771-2171 ext. 3523; fax: 886-2- 2731-49191; e-mail: asyang@ntut.edu.tw).

Yung-Chun Yang is with the School of Dentistry, National Defense Medical Center, Taipei 114, Taiwan (phone: 886-2-8792-3100; e-mail: juliemay2718@gmail.com).

Wen-Hsin Hsieh is with the Department of Mechanical Engineering, National Chung-Cheng University, Chiayi 621, Taiwan (phone: 886-5-2428170; fax: 886-5-2720589; e-mail: imewhh@ccu.edu.tw).

Chiang-Ho Cheng is with the Department of Mechanical and Automation Engineering, University of Dayeh, Changhua 51591, Taiwan (phone: 886-4-851-1888 ext. 2119; fax: 886-4-851-1224; e-mail: chcheng@mail.dyu.edu.tw).

with a high MFI (melt flow index, which is an index indicating how easy a thermoplastic polymer can melt and flow under a prescribed condition [16]. A higher MFI also suggests that COC has ideal properties for nanostructure transfer molding due to its polymer nature with low viscosity and high fluid mobility [17], [18]. The overall dimensions of COC sensor cover were 46 mm long. 22 mm wide, and 2 mm thick. The size of conventional micro channel was 29 mm (L) × 3 mm (W) × 0.2 mm (H), while the extents of modified cross-shaped micro channel was 15 mm (L) × 3 mm (W) × 0.2 mm (H). The optical sensor consisted of three sections: a micro channel, one inlet and one outlet for the liquid passage. It should be noted that the modified sensor design adopted two inlets and two outlets for minimizing the dispersion outcome. Micro channels were fabricated using the stainless steel mold installed on an electric-injection molding machine. Besides, the micro channel covers were also fabricated from COC by a similar process to the grating chips but replacing the stainless steel grating mold with a metallic mold of the micro channel.

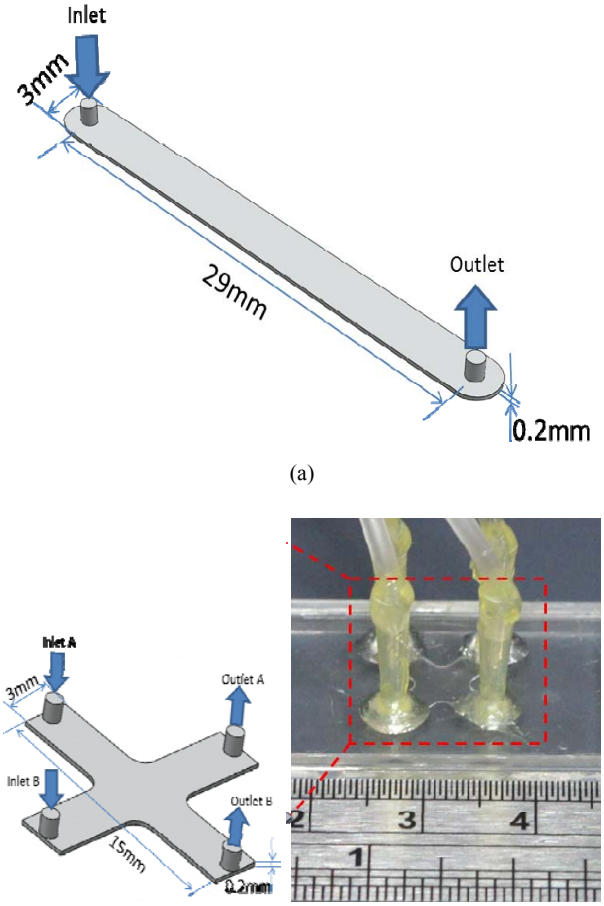

(a)

(b)

Fig. 1 Schematics and picture of optical sensors having (a) the conventional micro channel and (b) proposed cross-shaped micro channel

III. Experimental Apparatus

Fig. 3 exhibits the picture of the micro-flow visualization system for probing the dispersion event inside the microfluidic device. Two liquid samples were employed for studies: deionized (DI) water and DI water solution containing fluorescent dye (0.5% w/w Rhodamine 6G, Sigma-Aldrich). A syringe pump (NE-1600, New Era Pump Systems) was used to deliver controlled and continuous liquid sample flows into the device. The species concentration distributions were then characterized using the fluorescence technique with a 1-W semiconductor laser (L-532-1000A, Sintec Optronics Technology) having a beam diameter of ~1.0 mm and the wave length of 532-nm as a given excitation source. A fluorescence microscope (VMU-L, Mitutoyo) was utilized to acquire the optical visualized images of the illuminated flow pattern with high uniformity across the image plane. We used a 10×object lens (M plan APO NIR series, NA= 0.26, Mitutoyo) to gather fluorescence emissions, as well as a 570-nm high-pass filter (FGL570 Thorlabs) to isolate the shorter wavelength emissions from the comparatively weak fluorescent light for reducing the background noises. A charge-coupled device (CCD) camera (XC-HR57, SONY) was mounted on the microscope to snatch optical images, which were further processed by means of a data acquisition/analysis board (Domino Harmony, 64-bit, 66 MHz PCI, Euresys) and stored as a file on a personal computer. In fact, a linear relationship ensues between the fluorescence-dye concentration and the fluorescent intensity over a certain range [19]. Consequently, an empirical calibration procedure was utilized to transform the image intensities to concentration values. Those captured images were converted to gray-scale images with gray levels denoting fluid concentration contours. The experimental results from the obtained images can enhance the understanding of the dispersion flow process and establish a measurement database for model validation.

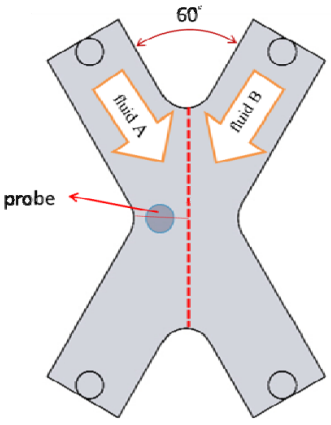

(a)

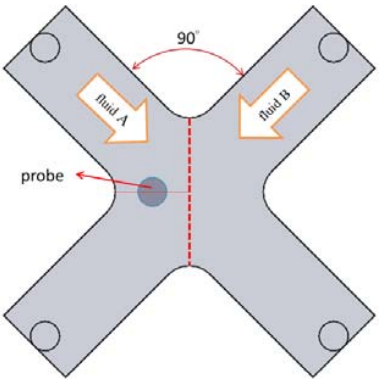

(b)

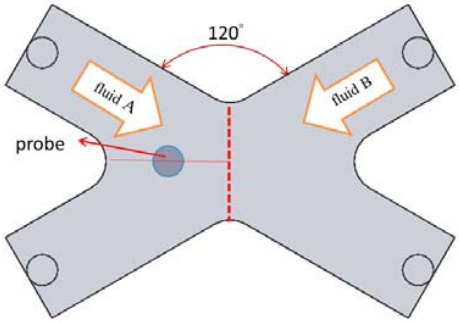

(c)

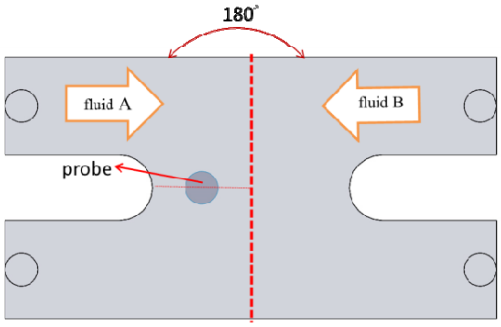

(d)

Fig. 2 Schematics of optical sensors with the designs of cross-shaped micro channel at angles of (a) 60°, (b) 90°, (c) 120° and (d) 180°

IV. Computational Analysis

A theoretical model built in the ANSYS/Fluent® software has been applied to examine the dispersion flow process in the proposed optical biosensor with a cross-shaped micro channel [20]. According to the experimental conditions, one test liquid was a solution containing fluorescent dye in DI water, and the other was DI water. In simulations, both fluids were treated as the incompressible, laminar, miscible, uniform-property liquid flows with the insignificant effects of gravity and temperature variation over the calculation domain. The model was based on the steady-state three-dimensional conservation equations of mass, momentum and species concentration described below:

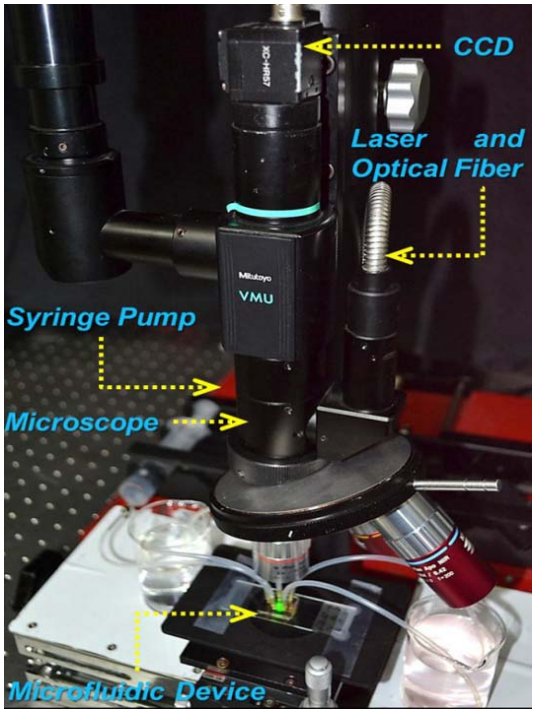

Fig. 3 Picture of the micro-flow visualization system

$$\frac{\partial u_i}{\partial x_i} = 0, \tag{1}$$

$$\frac{\partial(\rho u_i)}{\partial t} + \frac{\partial(\rho u_i u_j)}{\partial x_j} = -\frac{\partial p}{\partial x_i} + \frac{\partial}{\partial x_j}\left[\mu\left(\frac{\partial u_i}{\partial x_j} + \frac{\partial u_j}{\partial x_i}\right)\right], \tag{2}$$

$$\frac{\partial C}{\partial t} + \frac{\partial}{\partial x_j}(u_j C) = \frac{\partial}{\partial x_j}\left(D\frac{\partial C}{\partial x_j}\right). \tag{3}$$

The above variable u_i denotes the velocity component in the i direction; moreover, p, ρ, μ, D and C are the pressure, density, viscosity, binary diffusion coefficient and molar concentration of the species. The physical properties of pure water were applied to two test fluids with the associated ρ, μ and D values of 1000 kg/m^3, 0.001 N-s/m^2, and 10^{-10} m^2/s, respectively [21].

To characterize the transport behavior in the biosensor, the flow velocities of the incoming test fluids were specified as a uniform profile from the experiments or simulation conditions with the molar concentration of one of the fluid prescribed to 0 (DI water) and the other to 1 (DI water with fluorescent dye), respectively, at the inlets. The inflow velocity of the test fluids retained at 14 mm/s (200μL/s), corresponding to the Reynolds number (Re) of 80. In calculations, Re= $\rho V D_h/\mu$, and D_h is the hydraulic diameter of the micro channel. A fixed pressure of 1 atm was set at the flow outlet. The no-slip condition and zero normal gradients of pressure and concentration were imposed on all solid walls of the optical sensor. The above mathematical equations were further discretized into a set of cells using the finite control volume approach with an iterative semi-implicit method for pressure-linked equations consistent (SIMPLEC) numerical scheme implemented to couple the flow velocity and

pressure [22], [23].

V. Results and Discussion

Numerical simulations were conducted via the CFD software ANSYS/Fluent® to investigate the dispersion process inside the micro channels at different angles of the optical sensors. Fig. 4 illustrates the numerical grids of a cross-shaped micro channel at the angle of 90° for the baseline design. The mesh system included three major portions: the cross-shaped micro channel, inlet and outlet channels. Finer grids were placed in the areas near the cross junction of the channel and the wall boundaries with the mesh arranged to ensure orthogonality, smoothness and suitable aspect ratios to evade numerical divergence. The average cell length in the junction section was around 75 μm with the smallest spacing of 5.6 μm for resolving the steep variations of flow properties. During transient calculations, the normalized residual errors of flow variables converged to 10^{-5} with the mass balance check within 0.5% for each time step. The calculated velocity profiles along the transverse line of the cross junction at different grids (962536, 1299424 and 1780211) and CFL (0.2 and 0.5) values indicated that satisfactory grid independence could be achieved using a mesh setup of 1299424 grids with CFL= 0.5. A complete simulation for developing a dispersion flow field over the time interval of ~60 s (with the variation of steady surface concentrations at the sensing probe under 1%) generally necessitates around 100 hours of central processing unit (CPU) time on an Intel Core®i7 X900-3.47GHz (32 GB RAM) high-performance workstation.

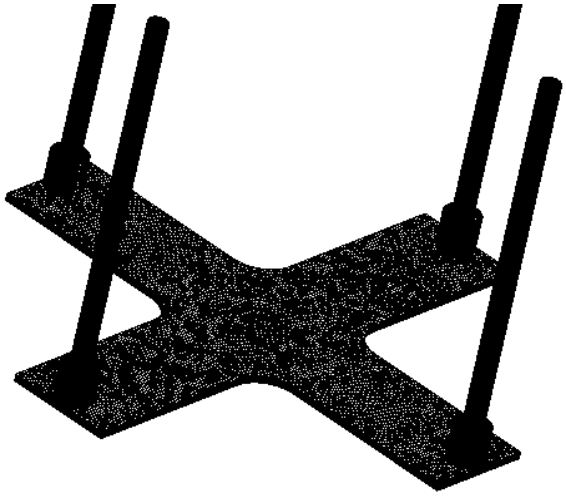

Fig. 4 Numerical grids of a cross-shaped micro channel at angle of 90° in a stereogram view

Fig. 5 demonstrates the predicted time sequences of the concentration iso-contours in (a) the conventional and (b) four cross-shaped micro channels at the angles of 60°, 90°, 120° and 180° of optical sensors. The probes were located at the center of the half width of the cross junction, as described in Fig. 2. To explore the dispersion process in the sensors, DI water (marked in a blue color) initially flowed through the micro channels at the incoming velocities of 14 mm/s to attain a stable flow condition. Afterwards, DI water with the dye (as the sample fluid marked in a red color) was introduced instantly at t= 0+ to replace the original pure water stream. The boundary of the sample stream was visualized via the concentration contour of C= 0.5 (marked in a yellow color) in the dispersion progression. For the case of the conventional micro channel, the sample fluid flowed into the micro channel from the inlet of the biosensor, progressively held more space during the time period of 0.2 — 15 s and reached to the outlet at 25s. Alternatively, throughout the time interval of 0.2– 4s, the sample fluid, supplied from the inlet of Fluid A, ran across the junction with a flow turning thanks to the transverse blockage of pure water from the other channel (Fluid B) and approached the outlet at t= 8s. When the sample fluid moved toward the junction, the fluid diffused with time along the moving direction. Meanwhile, the flow turning process around the junction tended to induce the non-uniform fluid velocity distribution, and thereby distort the concentration profile.

To assess the effectiveness of cross-shaped micro channels in minimizing dispersion, Fig. 6 exhibits the predicted surface concentrations at the sensing probe against time to appraise the influences of the dispersion in (a) the conventional and (b) four cross-shaped micro channels of the sensors. From the simulated results, the surface concentrations for the cases of cross-shaped micro channels essentially ascended to stable values in 9.2, 9.6, 10 and 10.8 s at the angles of 60°, 90°, 120° and 180°, whereas the sensor with the conventional channel required 38 s to reach its steady state. The sample stream met the DI water stream to develop a vertical stagnation plane in the middle of the cross junctions of the micro channels, the velocity of the sample fluid was accelerated due to contraction of the cross-sectional area, and in turn condensed the boundary layer thickness to achieve better concentration uniformity at the sensing probe. Therefore, dispersion was minimized owing to substantial decrease of the needed time duration by around four times toward the stable conditions when the design of cross-shaped micro channel was adopted.

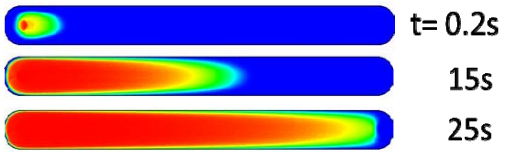

(a)

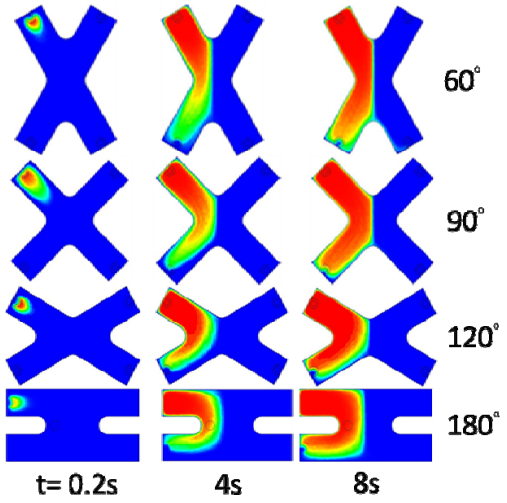

(b)

Fig. 5 Predicted time sequences of concentration contours in (a) the conventional; (b) four cross-shaped micro channels at different angles of optical sensors

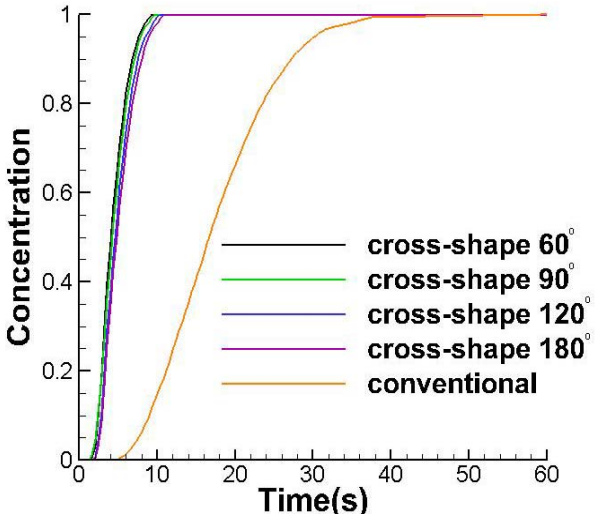

Fig. 6 Predicted surface concentrations at the sensing probe against time to appraise influences of dispersion in the conventional and four cross-shaped micro channels of optical sensors

VI. Conclusion

In this investigation, we proposed a new optical sensor using the design of cross-shaped micro channels to lessen dispersion. The CFD analysis was conducted to resolve the predicted time sequences of concentration contours for examining dispersion characteristics in the development of the modified cross-shaped micro channel pattern. To evaluate the influences of dispersion, we inspected the predicted surface concentrations at the sensing probe with respect to time. The simulated results revealed that the sample stream encountered the pure water stream to form a vertical stagnation plane in the middle of the cross junctions of micro channels for causing flow acceleration of the sample fluid, and thus reduced the boundary layer thickness to realize better concentration uniformity. As compared to the sensors with the typical micro channel, the proposed sensor design having the cross-shaped micro channel is capable of performing biological assays with less consumption amounts of bio-samples within a shorter period of test time.

Acknowledgment

This study represents part of the results obtained under the support of National Science Council, Taiwan, ROC (Contract No. NSC101-2221-E-027-148; 103-2221-E-194-016)

References

[1] R. Narayanaswamy, O. S. Wolfbeis, Optical Sensors, Springer, New York, 2004
[2] D. J. Bornhop, J. C. Latham, A. Kussrow, D. A. Markov, R. D. Jones, H. S. Sorensen, Free-solution label-free molecular interactions studied by back-scattering interfometry, Science 317 (2007) 1732–1736.
[3] M. J. Levene, J. Korlach, S. W. Turner, M. Foquet, H. G. Craighead, W. W. Web, Zeromode waveguides for single-molecule analysis at high concentrations, Science 299 (2003) 682–686.
[4] Y. Lin, F. Lu, Y. Tu, Z. Ren, Glucose biosensor based on carbon nanotube nanoelectrode ensembles, Nano Letters 4 (2004) 191–195.
[5] C. McDonagh, C.S. Burke, B.D. MacCraith, Optical chemical sensors, Chemical Reviews 108 (2008) 400–422
[6] J. Wang, Electrochemical glucose biosensors, Chemical Reviews 108 (2008)814–825.
[7] X. Fan, I. M. White, S. I. Shopova, H. Zhu, J. D. Suter, Y. Sun, Sensitive optical biosensor for unlabeled targets: a review, Analytica Chimica Acta 620 (2008)8–26.
[8] F. Vollmer, S. Arnold, Whispering-gallery-mode biosensing: laber-free detection down to single molecules, Nature Methods 5 (2008) 591–596.
[9] V. Goral et al, Label-free optical biosensor with microfluidics for sensing ligand-directed functional selectivity on trafficking of thrombin receptor, FEBS Letters 585 (2011) 1054–1060
[10] T. Kumeria et al, Label-free reflectometric interference microchip biosensor based on nanoporous alumina for detection of circulating tumour cells Biosensors and Bioelectronics 35 (2012) 167-173.
[11] X. Xu et al, A simple and rapid optical biosensor for detection of aflatoxin B1 based on competitive dispersion of gold nanorods, Biosensors and Bioelectronics 47 (2013) 361–367.
[12] L. Zhian et al Label-free biosensor by protein grating coupler on planar optical waveguides, optics letters Vol. 33, No. 15
[13] Robert Horvath et al, Grating coupled optical waveguide interferometer for label-free biosensing, Sensors and Actuators B 155 (2011) 446–450
[14] M. Matlosz et al. Micro channel reactors for kinetic measurement: Influence of diffusion and dispersion on experimental accuracy, Microreaction Technology
[15] N. Orgovan et al, In-situ and label-free optical monitoring of the adhesion and spreading of primary monocytes isolated from human blood: Dependence on serum concentration levels, Biosensors and Bioelectronics 54 (2014) 339–344
[16] J. Vlachopoulos et al, Polymer processing, Mater. Sci. Technol. Lond., 19 (2003), pp. 1161–1169
[17] S. H. Kim et al, Nanopattern insert molding, Nanotechnology 21(2010)
[18] R. R. Lamonte, D. McNally, Cyclic olefin copolymers, Adv. Mater. Process. 159 (2001)33–36.
[19] AWK. Law, H. Wang, Measurement of mixing processes with combined digital particle image velocimetry and planner laser induced fluorescence, Exp. Therm Fluid Sci. 22 (2000) 213-229.
[20] ANSYS/FLUENT, version 13 User guide manual, ANSYS Inc., Canonsburg, PA, USA, 2010 (Website: www.ansys.com).
[21] A. A. S. Bhagat, E. T. K. Peterson, I. Papautsky, A passive planar micro-mixer with obstructions for mixing at low Reynolds numbers, J. Micromech. Microeng. 17 (2007) 1017- 1024.
[22] J. P. Van Doormaal, G. D. Raithby, Enhancements of the SIMPLE method for predicting incompressible fluid flows, Numer. Heat Transfer 7 (1984) 147-163.
[23] D. S. Jang, R. Jetli, S. Acharya, Comparison of the PISO, SIMPLER, and SIMPLEC algorithms for the treatment of the pressure-velocity coupling in steady flow problems, Numer Heat Tran. 10 (1986) 209-228.

An-Shik Yang received his Bachelor of Science (1982) and Master of Science (1984) degrees from the National Tsing Hua University in Taiwan, and Ph.D. (1993) degree from the Pennsylvania State University in USA. He is currently a professor with the Dept. of Energy and Refrigerating Air-Conditioning Engineering at National Taipei University of Technology (NTUT) in Taipei,

Taiwan. Dr. Yang is an Associate Fellow of American Institute of Aeronautics and Astronautics (AIAA). His research interests include the microfluidic design, environmental fluid mechanics, and heat transfer.

Chin-Ting Kuo is currently pursuing the master degree in the Department of energy and refrigerating air-conditioning engineering from the National Taipei University of Technology, Taiwan. His primary research interests include the microfluidic device design, fluid dynamics, heat transfer and CFD simulation analysis.

Yung-Chun Yang is currently pursuing the medical degree at the School of Dentistry, National Defense Medical Center in Taipei, Taiwan. Her research interests include the oral diagnostic and pathology and periodontology and neuro-stem cells.

Wen-Hsin Hsieh received his Ph. D. in mechanical engineering from the Pennsylvania State University, University Park, PA, USA in 1987. He is currently a professor with the Department of Mechanical Engineering at National Chung Cheng University, Taiwan. His research interests are in the fields of bio-chip, microfluidics, combustion and heat transfer.

Chiang-Ho Cheng joins the Department of Mechanical and Automation Engineering at Dayeh University as an associate professor on February 1999, and was promoted to full professor in fall 2012. He earned his Ph.D. degree in Institute of Applied Mechanics from National Taiwan University in 1996. His research interests include the MEMS system, the integrated design and analysis of piezoelectric droplet inkjets and micropumps.